

THEORY
OF METALS

Effect of Mechanical Stresses on the Saturation Remanence of a System of Nanoparticles

L. L. Afremov^a and A. V. Panov^b

^a Far-East State University, ul. Sukhanova 8, Vladivostok, 690950 Russia

^b Institute of Automation and Control Processes, Far-East Division,
Russian Academy of Sciences, ul. Radio 5, Vladivostok, 690041 Russia

Received December 7, 2007

Abstract—Effect of mechanical stresses on the saturation remanence is investigated within the model of an ensemble of single-domain nanoparticles. It is shown that with increasing small uniaxial stresses the saturation remanence changes linearly. It is noted that an increase in tensile stresses leads to an increase in the longitudinal and decrease in the transverse remanence. The rate of change in the saturation remanence under the effect of a small longitudinal stress is half the appropriate rate of change in these characteristics in the transverse direction.

With increasing tensile stresses, the longitudinal saturation remanence reaches a maximum ($I_{rs}^{\parallel} > 0.5cI_s$) and then monotonically decreases to a certain limiting value. Compression leads to a monotonic decrease in I_{rs}^{\parallel} . The behavior of the transverse saturation remanence under the effect of a linear uniaxial tension (compression) is similar to the behavior of the longitudinal remanence during compression (tension). The results obtained agree well with the experiment.

PACS numbers: 75.75.+a, 75.80.+q

DOI: 10.1134/S0031918X08090020

1. INTRODUCTION

The investigations of the effects of mechanical stresses on the magnetic properties of natural and artificial magnetic materials have a more than half-century history. Thus, the results of an experimental study of the dependence of the initial susceptibility and different types of remanence on uniaxial stresses for igneous rocks and oceanic basalts can be found in [1–4], and for dolerites, in [5]. In [6–9], effects of mechanical loads on the magnetic properties of ferrites have been studied. A number of experimental works have been devoted to studying the effects of stress on the coercive force, initial susceptibility, and remanence of ferromagnetic steels [10–14].

This work is devoted to a theoretical investigation of the influence of mechanical stresses σ on the saturation remanence I_{rs} , but first we briefly consider the basic features of the experimental dependences of I_{rs} on σ .

At small compressive uniaxial stresses, the longitudinal saturation remanence arising in a magnetic field H parallel to the stresses σ decreases (and the transverse one increases) linearly [10, 12, 13]:

$$I_{rs}^{\parallel}(\sigma) = I_{rs}(1 - \beta_{rs}^{\parallel}\sigma); \quad I_{rs}^{\perp}(\sigma) = I_{rs}(1 + \beta_{rs}^{\perp}\sigma), \quad (1)$$

where I_{rs} is the saturation remanence in the absence of stresses; $\beta_{rs}^{\parallel} = |I_{rs}^{\parallel} - I_{rs}|/I_{rs}\sigma$ and $\beta_{rs}^{\perp} = |I_{rs}^{\perp} - I_{rs}|/I_{rs}\sigma$

are the rates of change in $I_{rs}(\sigma)$ arising due to stresses parallel and perpendicular to the magnetic field, respectively. For basalts, whose magnetic properties are determined by particles of oxidized titanomagnetites with sizes on the order of single-domain particles, the values of β_{rs}^{\parallel} and the ratio $r = \beta_{rs}^{\perp}/\beta_{rs}^{\parallel}$ are given in Table 1 [5]. Note that for the dolerites, whose matrix contains elongated particles of magnetite, the values of β_{rs}^{\parallel} in practice differ by an order of magnitude from the appropriate “basaltic” constants, while the ratio r differs only a little from the “basaltic” ones (see Table 1).

With increasing uniaxial tensile stresses parallel to the external magnetic field, the remanence of steels reaches maximum and then decreases, approaching a certain limit, while the uniaxial compression parallel to the external field leads to a monotonic decrease in remanence [10, 12, 13].

2. MAGNETIC STATES OF A CRYSTALLOGRAPHICALLY UNIAXIAL NANOPARTICLE

The states of the magnetic moment of a crystallographically uniaxial nanoparticle can be determined by

Table 1. Magnetic characteristics of oceanic basalts (samples with titanomagnetites $\text{Fe}_{3-x}\text{Ti}_x\text{O}_4$, nos. 238, 572D, 470A, 556, and 495) and dolerites (samples with magnetite, nos. 9144, 4305), fragment of Table 1 borrowed from [5] (for explanations, see the main text)

Characteristics	Sample						
	238	572D	470A	556	495	9144	4305
x	0.51	0.50	0.55	0.58	0.57	0	0
I_{rs}/I_s	0.44	0.45	0.43	0.50	0.35	0.45	0.42
$\beta_{rs}^{\parallel}, 10^{-9} \text{Pa}^{-1}$	2.76	2.21	4.58	2.52	3.70	0.65	0.68
$r = \beta_{rs}^{\perp}/\beta_{rs}^{\parallel}$	0.32	0.43	0.30	0.48	0.29	0.38	0.38

minimizing the free-energy density, which, if neglecting thermal excitations, takes the form

$$F = F(I_s^2) + \frac{1}{2}\beta_{ik}I_{sk}I_{si} + \frac{1}{2}N_{ik}I_{sk}I_{si} + \lambda_{iklm}\sigma_{il}I_{sk}I_{sm} \quad (2)$$

$$= F(I_s^2) + \frac{1}{2}(\beta_{ik} + N_{ik})I_{si}I_{sk} + \lambda_{iklm}\sigma_{il}I_{sk}I_{sm},$$

where β_{ik} , N_{ik} , λ_{iklm} , and σ_{il} are the tensors of uniaxial crystallographic anisotropy, demagnetizing factors, magnetostriction, and stresses, respectively (the repeated indices imply summing up). Taking into account that the tensors β_{ik} and N_{ik} in their principal

axes and in the related coordinate systems (x, y, z) and (x', y', z') have the form

$$\beta_{ik} \sim \begin{pmatrix} \beta_{11} & 0 & 0 \\ 0 & \beta_{22} & 0 \\ 0 & 0 & \beta_{33} \end{pmatrix}, \quad \beta_{22} = \beta_{33}; \quad (3)$$

$$N'_{ik} \sim \begin{pmatrix} N'_{11} & 0 & 0 \\ 0 & N'_{22} & 0 \\ 0 & 0 & N'_{33} \end{pmatrix}, \quad N'_{22} = N'_{33},$$

the tensor $\beta_{ik} + N'_{ik}$ can be written as

$$\beta_{ik} + N'_{ik} = \begin{pmatrix} B_{11} & (N'_{11} - N'_{22})\frac{\sin 2\alpha}{2} & 0 \\ (N'_{11} - N'_{22})\frac{\sin 2\alpha}{2} & B_{22} & 0 \\ 0 & 0 & \beta_{33} + N'_{33} \end{pmatrix}, \quad (4)$$

where $B_{11} = \beta_{11} + N'_{11}\cos^2\alpha + N'_{22}\sin^2\alpha$, $B_{22} = \beta_{22} + N'_{11}\sin^2\alpha + N'_{22}\cos^2\alpha$, and α is the angle between the axes x and x' . For a uniaxial crystal, the magnetoelastic part of the free-energy density can be converted to the form [15]

$$F_{ms} = -\hat{\lambda}_1\sigma_{11}I_{s1}^2 + \hat{\lambda}_2(\sigma_{22}I_{s2}^2 + \sigma_{33}I_{s3}^2) + (\hat{\lambda}_2 + \hat{\lambda}_3) \times \sigma_{23}I_{s2}I_{s3} - \hat{\lambda}_3(\sigma_{22}I_{s3}^2 + \sigma_{33}I_{s2}^2) - \hat{\lambda}_4(\sigma_{13}I_{s1}I_{s3} + \sigma_{12}I_{s1}I_{s2}), \quad (5)$$

where λ_i are the four magnetostriction constants of a uniaxial crystal and $\hat{\lambda}_i = \lambda_i/I_s^2$. In two special cases where the stresses are parallel to the plane (k_A, k_N) con-

taining the long axis of a grain of ellipsoidal shape and the axis of crystallographic anisotropy (making an angle β with the latter) (case *a*), and where the stresses are perpendicular to the plane (k_A, k_N) (case *b*), the expressions for the energy density can be written as follows.

In the case *a*, we have

$$F = F(I_s^2) - \frac{1}{4}I_s^2\sin^2\theta\{K\cos 2(\varphi - \gamma) + k_A + k_N + (\hat{\lambda}_1 - \hat{\lambda}_2 - 2\hat{\lambda}_3)\sigma + (\hat{\lambda}_1 + \hat{\lambda}_2 + 2\hat{\lambda}_3)\sigma\cos 2\beta\}, \quad (6)$$

where ϑ and φ are the polar coordinates of the vector of the spontaneous magnetization \mathbf{I}_s with the polar axis z perpendicular to the plane (k_A, k_N) ; the angles φ are measured from the axis of crystallographic anisotropy

(axis $\langle k_A \rangle$); $k_A = \beta_{22} - \beta_{11}$ and $k_N = N'_{22} - N'_{11}$ are the dimensionless constant of crystallographic anisotropy

and the constant of the shape anisotropy, respectively, which we assume to be positive

$$K = \sqrt{k_N^2 + 2k_N K_1 \cos(2\alpha - \psi_0) + K_1^2}; \quad (7)$$

$$\tan 2\gamma = \frac{k_N \sin 2\alpha + \hat{\lambda}_4 \sigma \sin 2\beta}{k_A + k_N \cos 2\alpha + (\hat{\lambda}_1 + \hat{\lambda}_2)\sigma + (\hat{\lambda}_1 - \hat{\lambda}_2)\sigma \cos 2\beta}; \quad (8)$$

$$K_1 = \sqrt{[k_A + (\hat{\lambda}_1 + \hat{\lambda}_2)\sigma + (\hat{\lambda}_1 - \hat{\lambda}_2)\sigma \cos 2\beta]^2 + [\hat{\lambda}_4 \sigma \sin 2\beta]^2}; \quad (9)$$

$$\tan \psi_0 = \frac{\hat{\lambda}_4 \sigma \sin 2\beta}{k_A + (\hat{\lambda}_1 + \hat{\lambda}_2)\sigma + (\hat{\lambda}_1 - \hat{\lambda}_2)\sigma \cos 2\beta}. \quad (10)$$

The analysis of expression (6) for the extremum shows that if the tensile or compressive stresses do not exceed a certain value σ_1^{\parallel} determined from the equation

$$K(\sigma_1^{\parallel}) + k_N + k_A + (\hat{\lambda}_1 - \hat{\lambda}_2 - 2\hat{\lambda}_3)\sigma_1^{\parallel} + (\hat{\lambda}_1 + \hat{\lambda}_2 + 2\hat{\lambda}_3)\sigma_1^{\parallel} \cos 2\beta = 0,$$

then at $\vartheta = \pi/2$, $\varphi = \gamma$, and at $\vartheta = \pi/2$, $\varphi = \pi + \gamma$ the free energy is minimum, while at $\vartheta = 0$, it is maximum. Thus, the ‘‘competition’’ of crystallographic anisotropy, shape anisotropy, and stresses leads to a uniaxial anisotropy with an effective anisotropy constant K and an effective axis oriented at an angle γ to the axis of the crystallographic anisotropy, along which the equilibrium magnetic moment of the nanoparticle becomes oriented.

The compressive stresses $|\sigma| > \sigma_1^{\parallel}$ ‘‘push out’’ the magnetic moment of the nanoparticle from the plane (k_A, k_N) , which becomes oriented perpendicular to it.

In the case *b*,

$$F = F(I_s^2) - \frac{1}{4} I_s^2 \sin^2 \theta \quad (11)$$

$$\times \{K \cos 2(\varphi - \gamma) + k_A + k_N + 2(\hat{\lambda}_3 + 2\hat{\lambda}_2)\sigma\};$$

$$K = \sqrt{(k_A - 2\hat{\lambda}_3\sigma)^2 + 2(k_A - 2\hat{\lambda}_3\sigma)k_N \cos 2\alpha + k_N^2}; \quad (12)$$

$$\tan 2\gamma = \frac{k_N \sin 2\alpha}{k_A + k_N \cos 2\alpha - 2\hat{\lambda}_3\sigma}. \quad (13)$$

At any compressive stresses or at tensile stresses $|\sigma| < \sigma_1^{\perp}$, where σ_1^{\perp} is a solution to the equation $K(\sigma_1^{\perp}) + k_N + k_A + 2(\hat{\lambda}_3 + 2\hat{\lambda}_2)\sigma_1^{\perp} = 0$, the magnetic moment of a nanoparticle in the equilibrium states is oriented along the effective axis ($\vartheta = \pi/2$, $\varphi = \gamma$ and $\vartheta = \pi/2$, $\varphi = \pi + \gamma$), which makes an angle γ with the axis of crystallo-

graphic anisotropy. The value of the effective anisotropy constant and the position of the effective axis in this case are determined by relationships (12), (13). Just as in the preceding case, the tensile stresses ($|\sigma| > \sigma_1^{\perp}$) push the magnetic moment of the nanoparticle out from the plane (k_A, k_N) , orienting it along the axis that becomes preferred due to the presence of stresses.

In an external magnetic field $F_H = -(\mathbf{H}, \mathbf{I}_s)$, the magnetic states of the nanoparticle are similar to the states of a uniaxial crystal with the following features:

1. If any tensile (or compressive) $|\sigma| < \sigma_2^{\parallel}$ stresses are parallel or if any compressive (or tensile) $|\sigma| < \sigma_2^{\perp}$ stresses are perpendicular to the plane (k_A, k_N) , then the critical field required for an irreversible rotation of the magnetic moment of a nanoparticle from the ‘‘against-the-field’’ state into the ‘‘along-the-field’’ state is determined by the effective anisotropy constant K (see relationships (7), (12), respectively): $H_0 = KI_s$.

Here, σ_2^{\parallel} and σ_2^{\perp} are the solutions to the equations

$$k_N + k_A + (\hat{\lambda}_1 - \hat{\lambda}_2 - 2\hat{\lambda}_3)\sigma_2^{\parallel} + (\hat{\lambda}_1 + \hat{\lambda}_2 + 2\hat{\lambda}_3)\sigma_2^{\parallel} \cos 2\beta - K(\sigma_2^{\parallel}) = 0;$$

$$k_N + k_A + 2(\hat{\lambda}_3 + 2\hat{\lambda}_2)\sigma_2^{\perp} - K(\sigma_2^{\perp}) = 0.$$

2. At $|\sigma| > \sigma_2^{\parallel}$ ($|\sigma| > \sigma_2^{\perp}$), the irreversible change in the magnetic moment of nanoparticle occurs after the external field H reaches a critical value H_0

$$H_0 = \frac{1}{2} I_s [K(\sigma) + k_N + k_A + (\hat{\lambda}_1 - \hat{\lambda}_2 - 2\hat{\lambda}_4)\sigma + (\hat{\lambda}_1 + \hat{\lambda}_2 + 2\hat{\lambda}_3)\sigma \cos 2\beta].$$

Note also that, depending on the applied stresses, the critical field $H_0 = KI_s$ can also change nonmonotonically. Thus, in the case *a* the critical field reaches minimum $H_{0\min} = |k_N I_s \sin(2\alpha - \psi_0)|$ at $K_1(\sigma) = -k_N \cos(2\alpha - \psi_0)$ (see relationships (9), (10)). In the case *b*, the critical

field becomes minimum ($H_{0\min} = k_N I_s \sin 2\alpha$ at $k_A - 2\hat{\lambda}_3 \sigma = -k_N \cos 2\alpha$).

3. MAGNETIC STATES OF A CRYSTALLOGRAPHICALLY MULTIAXIAL NANOPARTICLE

In the case where the uniaxial stresses σ are parallel to the plane of (k_A, k_N) , the equilibrium states of the magnetic moment of the nanoparticle whose crystal structure is cubic can be determined by minimizing the sum of densities of the magnetoelastic, magnetostatic, magnetocrystalline, and Zeeman free energies

$$F = F(I_s^2) - \frac{1}{4} I_s^2 \sin^2 \vartheta \times \{ 3\tilde{\lambda}_{100}(1 + \cos 2\varphi \cos 2\beta) + 3\tilde{\lambda}_{111} \sin 2\varphi \sin 2\beta \} \sigma + k_N(1 + \cos 2\alpha \cos 2\varphi + \sin 2\alpha \sin 2\varphi) - k_A(\sin^2 \vartheta \sin^2 2\varphi + 4 \cos^2 \vartheta) \} - (\mathbf{H}, \mathbf{I}_s), \quad (14)$$

where ϑ and φ are the polar coordinates of the vector of spontaneous magnetization \mathbf{I}_s reckoned from the axes $\langle 001 \rangle$ and $\langle 100 \rangle$, respectively; $\tilde{\lambda}_{100} = \lambda_{100}/I_s^2$; $\tilde{\lambda}_{111} = \lambda_{111}/I_s^2$; λ_{100} and λ_{111} are the magnetostriction constants; β is the angle between the axis $\langle 100 \rangle$ and the direction of mechanical stresses (applied parallel to the plane $\langle 100 \rangle$); and α is the angle between the axis $\langle 100 \rangle$ and the long axis of the ellipsoid, which is located in the plane $\langle 100 \rangle$.

If stresses are perpendicular to this plane ($\sigma \perp (k_A, k_N)$), then

$$F = F(I_s^2) - \frac{1}{4} I_s^2 \sin^2 \vartheta (3\tilde{\lambda}_{100}(1 + \cos 2\varphi) - k_A(\sin^2 \vartheta \sin^2 2\varphi + 4 \cos^2 \vartheta) + k_N(1 + \cos 2\alpha \cos 2\varphi + \sin 2\alpha \sin 2\varphi)) \} - (\mathbf{H}, \mathbf{I}_s). \quad (15)$$

The minimization of free energies (14), (15) leads to the following result: at all values of α , β , σ , k_A , and k_N which satisfy the condition

$$(k_N \cos 2\alpha + 3\lambda_{100} \sigma \cos 2\beta)^{\frac{2}{3}} + (k_N \sin 2\alpha + 3\lambda_{111} \sigma \sin 2\beta)^{\frac{2}{3}} > k_A^{\frac{2}{3}} \quad (16)$$

at the stresses σ parallel to the plane $\langle 100 \rangle$ and satisfy the condition

$$(k_N + 3\lambda_{100} \sigma) > k_A \quad (17)$$

at σ perpendicular to the plane $\langle 100 \rangle$, the nanoparticle is magnetically uniaxial.

For the majority of soft magnetic materials, relationships (16) and (17) are satisfied at an insignificant elon-

gation of nanoparticles. Thus, if the ratio of the major semiaxis to the minor semiaxis is $q = 1.1-1.2$, the shape-anisotropy constant is $k_N \approx 0.6-0.9$, whereas, e.g., $k_A \approx 0.16$ for iron, 0.2 for nickel, and 0.59 for magnetite. Thus, to analyze the magnetic states of nanoparticles we can use the results of the preceding section, i.e., to represent the expression for the free energy in the following form:

$$F = F(I_s^2) - \frac{1}{4} I_s^2 \sin^2 \vartheta \quad (18)$$

$$\times \{ 3\tilde{\lambda}_{100} \sigma + k_N + k_A + K \cos 2(\varphi - \gamma) \} - (\mathbf{H}, \mathbf{I}_s),$$

where at $k_A > 0$ the effective anisotropy constant K and the angle γ (which determines the position of the effective axis relative to the axis of $\langle k_A \rangle$ (parallel to $\langle 100 \rangle$)) are determined, depending on the mutual orientation of mechanical stresses, by relationships (20)–(25).

If $k_A < 0$, then the axis of crystallographic anisotropy $\langle k_A \rangle$ is the $\langle 111 \rangle$ axis. Therefore, for the analysis of states of the magnetic moment of a particle it is more convenient to use expression (18) after replacing ϑ and φ in it by Θ and Φ (the angles which determine the position of the magnetic moment of the particle relative to axis $\langle 111 \rangle$). These coordinates are connected as follows: $\cos \vartheta = \cos \Theta \cos \tilde{\Theta} + \sin \Theta \sin \tilde{\Theta} \cos(\Phi - \tilde{\Phi})$, $\varphi = \Phi + \pi/4$ ($\tilde{\Theta} = \arcsin \sqrt{2/3}$, $\tilde{\Phi} = \pi/4$ are the coordinates of the $\langle 111 \rangle$ axis relative to $\langle 001 \rangle$). In this case, just as in [16], the expression for the free-energy density can be reduced to the form

$$F = F(I_s^2) - \frac{1}{4} I_s^2 \cos^2 \left(\Phi - \frac{\pi}{4} \right) \times \left\{ - \frac{(\tilde{\lambda}_{100} + \tilde{\lambda}_{111}) \sigma}{2} + k_N + |k_A| + K \cos 2(\Theta - \gamma) \right\} - (\mathbf{H}, \mathbf{I}_s). \quad (19)$$

Here, just as above, K and γ are described by relationships (20)–(25).

In the case where the mechanical stresses are parallel to the plane which contains the $\langle k_A \rangle$ axis and the long axis of the ellipsoid, we have

$$K = \sqrt{k_N^2 + 2K_1 k_N \cos(2\alpha - \psi_0) + K_1^2}; \quad (20)$$

$$\tan 2\gamma = \frac{k_N \sin 2\alpha + \tilde{\lambda}_2 \sin 2\beta}{|k_A| + k_N \cos 2\alpha + \tilde{\lambda}_1 \sigma \cos 2\beta}; \quad (21)$$

$$K_1 = \sqrt{(|k_A| + \tilde{\lambda}_1 \sigma \cos 2\beta)^2 + (\tilde{\lambda}_2 \sigma \sin 2\beta)^2}, \quad (22)$$

$$\tan \psi_0 = \frac{\tilde{\lambda}_2 \sigma \sin 2\beta}{|k_A| + \tilde{\lambda}_1 \sigma \cos 2\beta};$$

where

$$\begin{aligned}\tilde{\lambda}_1 &= \begin{cases} 3\tilde{\lambda}_{100}, & k_A > 0, \\ (\tilde{\lambda}_{100} + 5\tilde{\lambda}_{111})/2, & k_A < 0, \end{cases} \\ \tilde{\lambda}_2 &= \begin{cases} 3\tilde{\lambda}_{111}, & k_A > 0, \\ 2\tilde{\lambda}_{100} + \tilde{\lambda}_{111}, & k_A < 0. \end{cases}\end{aligned}\quad (23)$$

In the second case (mechanical stresses are applied perpendicular to the plane containing the $\langle k_A \rangle$ axis and the long axis of the ellipsoid), we obtain

$$K = \sqrt{k_N^2 + 2k_N(|k_A| + \tilde{\lambda}_1\sigma)\cos 2\alpha + (|k_A| + \tilde{\lambda}_1\sigma)^2}; \quad (24)$$

$$\tan 2\gamma = \frac{k_N \sin 2\alpha}{|k_A| + k_N \cos 2\alpha + \tilde{\lambda}_1\sigma}. \quad (25)$$

In the absence of a magnetic field, the equilibrium positions of the magnetic moment of the grain at $k_A > 0$ coincide with the position of the effective axis: $\vartheta = \pi/2$, $\varphi = \gamma$, and $\vartheta = \pi/2$, $\varphi = \pi + \gamma$. These states have identical free energies $F = F(I_s^2) - I_s^2(3\tilde{\lambda}_{100}\sigma + k_N + k_A + K)/4$.

The equilibrium states of the magnetic moment (effective axis) of the particle relative to the $\langle 111 \rangle$ axis are determined in a similar way at $k_A < 0$: $\Theta = \gamma$, $\Phi = \pi/4$ and $\Theta \approx \pi + \gamma$, $\Phi = \pi/4$. The maximum critical field of the irreversible change in the magnetic moment of the grain H_0 can be determined by minimizing expressions (18), (19).

In the first case ($\sigma \parallel H$), this field is equal to

$$H_0 = I_s \sqrt{k_N^2 + 2k_N K_1 \cos(2\alpha - \psi_0) + K_1^2}; \quad (26)$$

in the second case ($\sigma \perp H$), we have

$$H_0 = I_s \sqrt{k_N^2 + 2k_N(|k_A| + \tilde{\lambda}_1\sigma)\cos 2\alpha + (|k_A| + \tilde{\lambda}_1\sigma)^2}. \quad (27)$$

A specific feature of relationships (26), (27) is the nonmonotonic dependence of H_0 on the shape anisotropy. If $\sigma \parallel H$, then with increasing k_N the critical field reaches minimum $H_{0\min} = K_1 I_s \sin(2\alpha - \psi_0)$ at $k_N = -K_1 \cos(2\alpha - \psi_0)$. If $\sigma \perp H$, the minimum critical field $H_{0\min} = I_s(|k_A| + \tilde{\lambda}_1\sigma)\sin 2\alpha$ is reached when $k_N = -(|k_A| + \tilde{\lambda}_1\sigma)\cos 2\alpha$.

In the system of particles which have different elongation, the spectrum of critical fields should apparently be distributed from $H_{0\min}$ to $H_{0\max} = I_s(k_A + k_N)$. In view of the symmetry of relationships (26) and (27) relative

to k_N and $K_1 = K_1(\sigma)$, the dependence of H_0 on mechanical stresses is also nonmonotonic with respect to $K_1 = K_1(\sigma)$.

4. SATURATION REMANENCE

Model:

1. We consider an ensemble of N single-domain noninteracting magnetic nanoparticles, which have the form of prolate ellipsoids of rotation, embedded in a nonmagnetic matrix.

2. The axis that becomes preferred due to the effect of crystallographic anisotropy (axis $\langle k_A \rangle$) makes an angle α with the major axis of the ellipsoid.

3. The uniaxial mechanical stresses σ make an angle β with the axis $\langle k_A \rangle$ if they are applied in the plane (k_A, k_N) which includes the major axis of the ellipsoid and the axis $\langle k_A \rangle$, or if stresses σ are perpendicular to this plane.

For the evaluation of the effect of mechanical stresses σ on the residual saturation magnetization I_{rs} , we will use the above-described model of single-domain particles whose axes of crystallographic anisotropy will be considered to be parallel to the major axes of the ellipsoids. According to (8) and (21), the position of the effective axis relative to the axis of crystallographic anisotropy $\langle k_A \rangle$ will be determined by the following relationship:

$$\tan 2\gamma = \frac{\Lambda_2 \sigma \sin 2\beta}{k + \Lambda_1 \sigma \cos 2\beta}, \quad (28)$$

where the positive values of σ correspond to tensile stresses, and the negative values, to compressive stresses:

$$\begin{aligned}\Lambda_1 &= \begin{cases} \hat{\lambda}_1 - \hat{\lambda}_2, \\ \tilde{\lambda}_1, \end{cases} & \Lambda_2 &= \begin{cases} \hat{\lambda}_4, \\ \tilde{\lambda}_2, \end{cases} \\ k &= \begin{cases} |k_A| + k_N + (\hat{\lambda}_1 + \hat{\lambda}_2)\sigma; \\ |k_A| + k_N. \end{cases}\end{aligned}\quad (29)$$

Here, the upper line gives the constants of a uniaxial crystal, and the lower line, of a multiaxial crystal.

If θ and φ are the polar coordinates of the vector of spontaneous magnetization \mathbf{I}_s relative to the vector of external field \mathbf{H} , then the projection of the residual saturation magnetization on the direction of \mathbf{I} can be determined as follows:

$$I_{rs}^{(l)} = \int_0^{2\pi} d\varphi \int_0^{\pi/2} 2mc \cos p(\theta, \varphi) F(\theta, \varphi) d\theta. \quad (30)$$

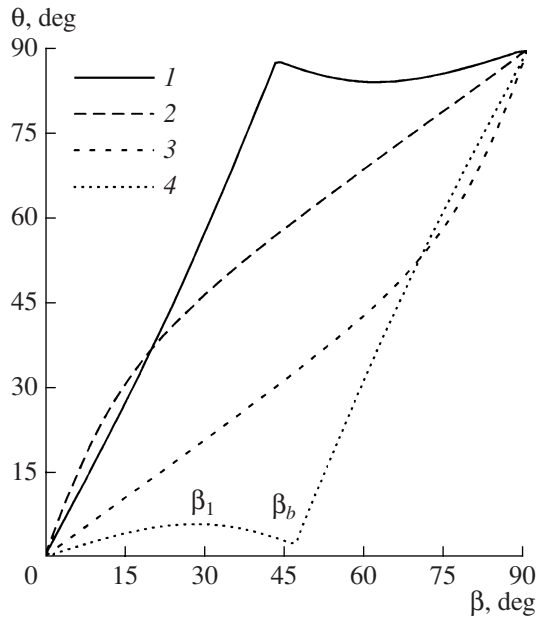


Fig. 1. The $\theta(\beta)$ dependence at $k_N = 0$ for magnetite particles: (1) $\sigma = -10^9$ Pa; (2) -5×10^7 Pa; (3) 5×10^7 Pa; and (4) 10^9 Pa.

Here, $m = I_s v$; I_s and v are the magnetic moment and the volume of the particle; c is the volume concentration of particles; $p(\theta, \varphi)$ is the angle between the vector \mathbf{l} and the magnetic moment of the particle; and $F(\theta, \varphi)$ is the distribution function of magnetic moments relative to the magnetic field \mathbf{H} .

Assuming the chaotic distribution over $\beta - f(\beta) = \sin\beta/4\pi$, the distribution function $F(\theta, \varphi)$ can be con-

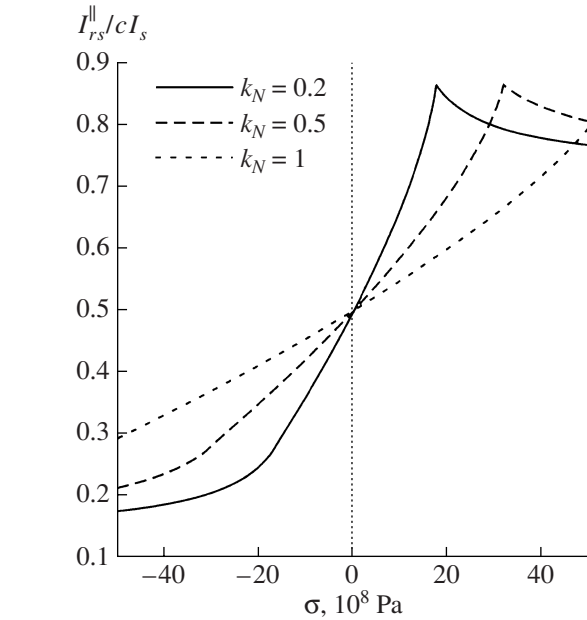


Fig. 2. Dependence of I_{rs}^{\parallel} of the ensemble of single-domain particles of steel on the magnitude of stresses for different values of the shape anisotropy.

structed as follows: $F(\theta, \varphi) = f(\beta(\theta), \alpha(\varphi)) |d\beta/d\theta| d\alpha/d\varphi$, where $\alpha = \varphi$, and $\beta = \beta(\theta)$ is expressed from relationship (31)

$$\theta = \beta - \gamma = \beta - \frac{1}{2} \arctan \frac{\Lambda_2 \sigma \sin 2\beta}{|k + \Lambda_1 \sigma \cos 2\beta|}. \quad (31)$$

By differentiating (31), we obtain

$$\frac{d\beta}{d\theta} = \left(\frac{d\theta}{d\beta} \right)^{-1} \equiv \Psi(\theta) = \left\{ 1 - \frac{\Lambda_2 \sigma [\Lambda_1 \sigma + (|k_A| + k_N) \cos 2\beta(\theta)] \operatorname{sgn}[|k_A| + k_N + \Lambda_1 \sigma \cos 2\beta(\theta)]}{[|k_A| + k_N + \Lambda_1 \sigma \cos 2\beta(\theta)]^2 + [\Lambda_2 \sigma \sin 2\beta(\theta)]^2} \right\}^{-1}. \quad (32)$$

Thus, the longitudinal saturation remanence is

$$I_{rs}^{\parallel} = c I_s \int_0^{\pi/2} |\Psi(\theta)| \sin \beta(\theta) \cos(\theta) d\theta. \quad (33)$$

Analogously, it is possible to calculate the transverse magnetization:

$$I_{rs}^{\perp} = \frac{c I_s}{2\pi} \int_0^{2\pi} d\tilde{\varphi} \int_0^{\pi/2} |\Psi(\theta)| \sin \beta(\theta) \cos \tilde{\theta} d\tilde{\theta}, \quad (34)$$

where $\tilde{\theta}$ and $\tilde{\varphi}$ are the polar and azimuthal coordinates of the effective axis relative to the direction \mathbf{l} , which are connected with θ as follows:

$$\cos \theta = \sin \tilde{\theta} \cos \tilde{\varphi}.$$

When integrating relationships (33), (34), it is necessary to consider the ambiguity of the $\beta(\theta)$ dependence at $|\sigma| > (|k_A| + k_N)/\Lambda_1$ (Fig. 1). If $\sigma > (|k_A| + k_N)/\Lambda_1$, the integration should be conducted in the limits $(0, \beta_1), (\beta_1, \beta_b), (\beta_b, \pi/2)$; for $\sigma < -(|k_A| + k_N)/\Lambda_1$, in the limits $(0, \beta_b), (\beta_b, \beta_1), (\beta_1, \pi/2)$, where

$$\beta_b = \frac{\pi}{2} - \frac{1}{2} \arccos \frac{|k_A| + k_N}{\Lambda_1 \sigma};$$

$$\beta_1 = \frac{\pi}{2} - \frac{1}{2} \arccos \frac{-2A + (2\Lambda_1 - \Lambda_2)(|k_A| + k_N)}{2(\Lambda_1^2 - \Lambda_2^2)\sigma};$$

$$A = \sqrt{\Lambda_2 \left[(\Lambda_1 - \Lambda_2)^2 (\Lambda_1 + \Lambda_2) \sigma^2 + (|k_A| + k_N) \left(\frac{5}{4} \Lambda_2 - \Lambda_1 \right) \right]}.$$

In the approximation $\Lambda_1 \sigma, \Lambda_2 \sigma \ll (|k_A| + k_N) I_s$, relationship (33), (34) can be reduced to the form

$$I_{rs}^{\parallel} = \frac{c I_s}{2} \left[1 + \frac{\Lambda_2 \sigma}{2k} \right], \quad (35)$$

$$I_{rs}^{\perp} = \frac{c I_s}{2} \left[1 - \frac{\Lambda_2 \sigma}{4k} \right]. \quad (36)$$

Relationships (33), (34) determine the theoretical dependence of the saturation remanence on stresses, which is displayed in Figs. 2 and 3.

5. DISCUSSION

The increase in the saturation remanence I_{rs}^{\perp} and the decrease in I_{rs}^{\parallel} with increasing compressive stresses are connected with the dependence of the orientation of the effective axis on σ . According to (28), the compressive stresses parallel to the magnetic field \mathbf{H} increase the

angle between \mathbf{H} and the effective axis, which leads to a decrease in the projection of the magnetic moment on the field direction and, therefore, to a decrease in I_{rs}^{\parallel} as well. Correspondingly, the compressive stresses perpendicular to the field decrease the angle between the effective axis and the field, which must lead to the following relationship between the magnetizations: $I_{rs}^{\parallel} < I_{rs}^{\perp}$, which is indeed observed experimentally upon compression.

According to (35), (36), in the region of small stresses ($\Lambda_1 \sigma, \Lambda_2 \sigma \ll k$), an increase in the compression leads to a linear increase in I_{rs}^{\perp} (decrease in I_{rs}^{\parallel}) relative to σ ; moreover, the rate of change in the longitudinal saturation remanence $\beta_{rs}^{\parallel} = \Lambda_2 / (2(|k_A| + k_N))$, being twice the rate $\beta_{rs}^{\perp} = \Lambda_2 / (4(|k_A| + k_N))$ of change in the transverse remanence, depends on the relationship between the magnetostriction constants, crystallographic anisotropy, and shape anisotropy, which agree well with the results of the theoretical studies [17].

Let us compare the experimental values of β_{rs}^{\parallel} for steels with the theoretical ones. According to [10], for a mild steel we have $\beta_{rs}^{\parallel} = 2 \times 10^{-9} \text{ Pa}^{-1}$; for a structural steel [12], it is lower by almost an order of magnitude and, depending on the temperature of annealing, takes on the following values: $\beta_{rs}^{\parallel} = (0.3-0.6) \times 10^{-9} \text{ Pa}^{-1}$.

The calculation of the rate of change in I_{rs}^{\parallel} carried out for the nanoparticles of steel shows that, depending on the elongation of the nanoparticle (almost spherical ($k_N = k_A$) or infinitely elongated ($k_N = 4\pi$)) – β_{rs}^{\parallel} takes on values in the limits from 0.3×10^{-9} to $0.06 \times 10^{-9} \text{ Pa}^{-1}$. When calculating β_{rs}^{\parallel} , we used the experimental fact of the positivity of the magnetostriction constants of steels [18–20], which made it possible to assume that $\lambda_{100} \approx \lambda_{111} = 20 \times 10^{-6}$. The constants of crystallographic anisotropy and saturation magnetization were taken equal to the appropriate constants of iron, i.e., $k_A = 0.16$, $I_s = 1710 \text{ kA/m}$ [21].

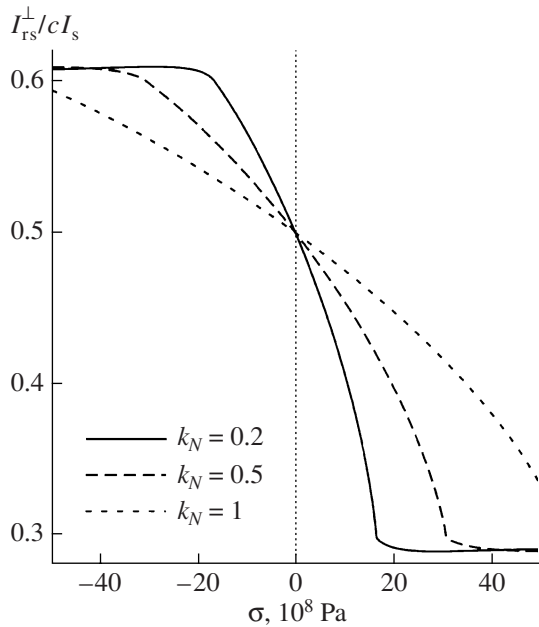


Fig. 3. Dependence of I_{rs}^{\perp} of the ensemble of single-domain particles of steel on the magnitude of stresses for different values of the shape anisotropy.

Table 2. Theoretical values of the slopes of the dependences of the saturation remanence on the stress for titanomagnetites $\text{Fe}_{3-x}\text{Ti}_x\text{O}_4$ ($\beta_{rs \min}^{\parallel}$ corresponds to the elongated particles ($k_N = 4\pi$); $\beta_{rs \max}^{\parallel}$, to $k_N = k_A$; K_1 is the constant of magnetic crystallographic anisotropy)

x	0	0.04	0.1	0.18	0.31	0.56
I_s , kA/m [22]	480	468	426	380	307	151
K_1 , 10^4 J/m ³ [22]	-1.36	-1.96	-2.50	-1.92	-1.81	-0.70
λ_{100} , 10^{-6} [22]	-20	-6	4	47	67	170
λ_{111} , 10^{-6} [22]	78	87	96	109	104	92
$\beta_{rs \min}^{\parallel}$, 10^{-9} Pa ⁻¹	0.06	0.13	0.21	0.51	0.87	6.1
$\beta_{rs \max}^{\parallel}$, 10^{-9} Pa ⁻¹	0.70	0.96	1.0	2.6	3.3	15

Note also that the rate of change in $I_{rs}^{\parallel}(\sigma)$ calculated for the system of very elongated ($k_N = 6$) particles of $\text{Fe}_{2.44}\text{Ti}_{0.56}\text{O}_4$ ($\beta_{rs}^{\parallel} = 4 \times 10^{-9}$ Pa⁻¹) only insignificantly differs from the experimental values of β_{rs}^{\parallel} for close-in-composition titanomaghemite-containing basalts (see Table 1). The same conclusions can be referred also to magnetite-containing dolerites (see Table 1), for which, depending on the elongation of particles ($k_N = k_A$ or $k_N = 4\pi$), the calculated values of β_{rs}^{\parallel} ($\beta_{rs \min}^{\parallel}$, $\beta_{rs \max}^{\parallel}$, respectively, see Table 2) differ by more than an order of magnitude.

As was noted above, it follows from relationships (35), (36) that β_{rs}^{\parallel} must be twice as large as β_{rs}^{\perp} . This relationship is in accordance with the results of experiment [5]. If we assume the equality $I_{rs}/I_s = 0.5$ as the criterion of single-domain structure, then particles embedded in the basaltic sample no. 556 can be referred to single-domain ones. For this sample, $r = \beta_{rs}^{\perp}/\beta_{rs}^{\parallel} = 0.48$ (see Table 1).

With increasing tensile stresses (see Fig. 2), the longitudinal saturation remanence I_{rs}^{\parallel} increases, reaching a maximum value $I_{rs \max}^{\parallel} > 0.5cI_s$ at $\sigma_m = (|k_A| + k_N)/\tilde{\lambda}_1$ and then monotonically decreases to $I_{rs}^{\parallel}|_{\sigma \rightarrow +\infty} \approx 0.31cI_s$. Such a behavior of I_{rs}^{\parallel} is determined by the dependence of the position of the effective axis on the stress (see (28)). At $\sigma \rightarrow \sigma_m$, the effective axes of particles with $0 < \beta < \pi/4$ are oriented at an angle $\gamma < \beta$ to the field \mathbf{H} , and of the axes of particles with $\pi/4 < \beta < \pi/2$, at an angle of $\gamma \rightarrow \pi/4$: I_{rs}^{\parallel} reaches maximum. A further increase in the stress will lead to an increase in the angle γ ($\gamma > \beta$) for the particles with $\pi/4 < \beta < \pi/2$, which corresponds to a decrease in the projection of magnetization and I_{rs}^{\parallel} , respectively.

The decrease in I_{rs}^{\parallel} upon compression is determined by an increase in the deviation of the effective axes of all particles relative to the field \mathbf{H} . For this very reason $I_{rs}^{\parallel}|_{\sigma \rightarrow -\infty} < I_{rs}^{\parallel}|_{\sigma \rightarrow +\infty}$.

The transverse saturation remanence I_{rs}^{\perp} , in contrast to I_{rs}^{\parallel} , is measured in the direction perpendicular to σ ; therefore, an increase in the deviation of the effective axis caused by tensile stresses leads to a decrease in the projection of the magnetic moment on the field direction. The presence of a minimum in the $I_{rs}^{\perp} = I_{rs}^{\perp}(\sigma)$ curve is caused by above-described effect of orientation of the effective axes of all particles with $\pi/4 < \beta < \pi/2$ at an angle $\gamma = \pi/4$ at $\sigma \rightarrow \sigma_m$.

The absence of the dependence of the saturation remanences I_{rs}^{\parallel} and I_{rs}^{\perp} on the total anisotropy is connected with the fact that the orientation of the effective axes are independent of this anisotropy at $\sigma \gg \sigma_m$:

$$\text{according to (28), } \tan 2\gamma = \frac{\tilde{\lambda}_2}{\lambda_1} \tan 2\beta.$$

This theoretical dependence of the saturation remanence on the stresses does not qualitatively contradict the results of the experimental studies of I_{rs}^{\parallel} of soft [10, 14] and structural steels [12, 13].

REFERENCES

1. A. G. Kalashnikov and S. P. Kapitsa, "Magnetic Susceptibility of Rocks under Elastic Stresses," Dokl. Akad. Nauk SSSR **86** (3), 521–523 (1952).
2. S. P. Kapitsa, "Magnetic Properties of Igneous Rocks under Mechanical Stresses," Izv. Akad. Nauk SSSR, Ser. Geofiz., No. 6, 489–504 (1955).
3. T. Nagata and H. Kinoshita, "Studies on Piezo-Magnetization (I) Magnetization of Titaniferous Magnetite under Uniaxial Compression," J. Geomagn. Geoelectr. **17** (2), 121–135 (1965).

4. T. Nagata, "Basic Magnetic Properties of Rocks under the Effect of Mechanical Stresses," *Tectonophysics* **9** (2–3), 167–195 (1970).
5. J. P. Hodych and J. Matzka, "Saturation Magnetostriction and Its Low-Temperature Variation Inferred for Natural Titanomagnetites: Implications for Internal Stress Control of Coercivity in Oceanic Basalts," *Geophys. J. Int.* **157**, 1017–1026 (2004).
6. N. Sirota and Yu. Khachatryan, "The Effect of Hydrostatic Pressure on the Magnetic Susceptibility of Cu–Zn Ferrites," *Fiz. Tverd. Tela* **5** (11), 3110–3112 (1963).
7. M. Le Floch, J. Loaec, H. Pascard, and A. Globus, "Effect of Pressure on Soft Magnetic Materials," *IEEE Trans. Magn.* **17** (6), 3129–3132 (1981).
8. A. Bieńkowski and J. Kulikowski, "The Effect of Stresses on Magnetized Ni–Zn(Co) Ferrite Cores," *Phys. Scr.* **44**, 379–381 (1991).
9. A. Bieńkowski, "Magnetoelastic Villari Effect in Mn–Zn Ferrites," *J. Magn. Magn. Mater.* **215–216**, 231–233 (2000).
10. R. Langman, "Magnetic Properties of Mild Steel under Conditions of Biaxial Stress," *IEEE Trans. Magn.* **26** (4), 1246–1251 (1990).
11. V. Zakharov, M. Borovkova, and V. Komarov, "Effect of External Stresses on the Coercive Force of Carbon Steels," *Defektoskopiya*, No. 1, 41–46 (1992).
12. E. Gorkunov, T. Tsar'kova, S. Smirnov, et al., "Effect of Deviation from Coaxiality between the Directions of Magnetization and Mechanical Strain on the Results of Magnetic Testing of Elastic Strain in Steels" *Defektoskopiya* **40** (5), 40–52 (2004) [*Russ. J. Nondestr. Test.* **40** (5), 317–325 (2004)].
13. V. G. Kuleev, T. P. Tsar'kova, A. P. Nichipuruk, et al., "On the Origin of Essential Differences in the Coercive Force, Remanence, and Initial Permeability of Ferromagnetic Steels in the Loaded and Unloaded States upon Plastic Tension" *Fiz. Met. Metalloved.* **103** (2), 136–146 (2007) [*Phys. Met. Metallogr.* **103** (2), 131–141 (2007)].
14. C. S. Schneider, "Effect of Stress on the Shape of Ferromagnetic Hysteresis Loops," *J. Appl. Phys.* **97**, 10E503, (2005).
15. S. V. Vonsovskii and Ya. S. Shur, *Ferromagnetism* (Gostekhizdat, Moscow, 1948) [in Russian].
16. F. D. Stacey and M. J. S. Johnston, "Theory of the Piezomagnetic Effect in Titanomagnetite-Bearing Rocks," *Pure Appl. Geophys.* **97** (5), 146–155 (1972).
17. M. J. Sablik, S. W. Rubin, L. A. Riley, et al., "A Model for Hysteretic Magnetic Properties under the Application of Noncoaxial Stress and Field," *J. Appl. Phys.* **74** (1), 480–488 (1993).
18. B. V. Molotilov and L. B. Kazadzhani, "Magnetic Properties and Structure of Transformer Steels," *Metalloved. Term. Obrab. Met.*, No. 6, 52–58 (1966).
19. A. P. Kovalenko, F. D. Miroshnichenko, E. A. Prokopchenko, et al., "Effect of Elastic Strains on the Initial Permeability of Transformer Steel Coated with a Nickel Film," *Izv. Vyssh. Uchebn. Zaved., Fiz.* **11** (12), 134–135 (1968).
20. V. G. Kanibolotskii, F. D. Miroshnichenko, and V. L. Snezhnoi, "Mechanical Properties of KH15N5D2T Steel after Heat Treatment," *Metalloved. Term. Obrab. Met.*, No. 5, 63–64 (1972).
21. S. Chikazumi, *Physics of Ferromagnetism. Vol. 2. Magnetic Characteristics and Practical Applications* (Syokabo, Tokyo, 1984; Mir, Moscow, 1987).
22. Y. Syono, "Magnetocrystalline Anisotropy and Magnetostriction of FeO₄–Fe₂TiO₄ Series with Special Application to Rock Magnetism," *Jpn. J. Geophys.* **4** (1), 71–143 (1965).